J. Membrane Biol. 98, 1–13 (1987)

The Journal of
Membrane Biology

I/V-Curve Studies of the Control of a K^+ Transporter in *Nitella* by Temperature

Ulf-Peter Hansen and Joachim Fisahn
Institut für Angewandte Physik, Neue Universität, 2300 Kiel, Federal Republic of Germany

Summary. In *Nitella*, current-voltage relationships were measured at different temperatures ranging from 5 to 25°C. Sets of these *I/V* curves were subject to curve fitting on the basis of a cyclic reaction scheme (Class I model). Different hypotheses of the mode of action of temperature on the *I/V* curve were tested, including changes in reaction constants in the transport cycle and deactivation of transport molecules. It was found that models assuming an influence of temperature on pairs of rate constants of the transport cycle gave very bad fits. Good fits were obtained with models implying that temperature influences the number of active transporters. The lazy-state model (the exchange of an inactive state with a state N_3 in the transport cycle is influenced by temperature) gave a slightly better fit than the assumption of an unspecific inactivation (independent of the state of the transport molecule). According to the lazy-state analysis, the inactive state is kinetically closer to N_o, the state in which the transport molecule is open to the outside substrate than to N_i, the state in which it is open to the inside substrate. The two inactivation models imply that temperature does not act directly on the properties of the plasmamembrane, but that temperature-sensitive metabolic processes in the cell send signals which control the activation and deactivation of the transporter.

Key Words control · curve fitting · *I/V* curves · K^+ transporter · *Nitella* · lazy state · reaction-kinetic model · temperature

Introduction

The occurrence of oscillations (Fisahn, Mikschl & Hansen, 1986) revealed the involvement of control processes in the activation and deactivation of membrane transporters. Further evidence for the importance of these control processes was obtained from the analysis of the temperature effect on membrane potential and on resistance (Fisahn & Hansen, 1986).

An estimate of the nature of the temperature-induced changes can be obtained from what may be called the *RT/F* component. All equations of the electrical characteristics of membrane transport start with the factor *RT/F*. This factor introduces an obvious temperature dependence, the *RT/F* component. In the investigations of Fisahn and Hansen (1986), the responses to fast changes in temperature (shorter than 1 sec) obtained the values predicted by the *RT/F* component. However, slow changes caused much greater signals. Either of these features, the magnitude of the responses or the occurrence of slow time constants (20 sec to 10 min) indicates that transport activity is subject to control by signals from other temperature-sensitive functional units of the cell.

In the case of the temperature-induced changes in membrane potential, which are assigned to the electrogenic H^+ pump, the time constants obtained from the kinetic analysis were found to be equal to those of the light-induced changes in membrane potential. Consequent upon this, the statement was obtained that the temperature effects on photosynthesis and on cytoplasmic pH regulation, and not the temperature effect on this transporter itself, controlled the activity of the electrogenic pump.

Also, the biochemical mechanism related to the time constant of the temperature action on resistance which is assigned to a K^+ channel, seems to be located in the chloroplasts as seen from recent (*unpublished*) studies of Susanne Stein in our laboratory. She found that the time constants of the temperature effect on resistance (and on potential) are very sensitive to light intensity. This implies that the reactions sending the signal to the K^+ channel "see" the light, i.e., the concentrations of the involved reactants vary strongly with light intensity. Thus, also in the case of the temperature effect on resistance the involvement of control mechanisms rather than a direct effect of temperature has to be assumed.

The question which could not be answered in the preceding paper is that of the mechanism by means of which the signals from the temperature-modulated metabolic processes manage to control transport activity. Two different modes can be imagined: slowing down of the reactions in the transport cycle (catalytic effect) or complete deactivation of some transport molecules.

Models and evidence for the control of transport activity by transitions into and out of an inactive (lazy) state have been obtained from the study of the temporal behavior of membrane transport. Hansen, Tittor and Gradmann (1983) calculated the influence of the exchange with the "lazy state" on transport activity. Warncke and Lindemann (1985) explained the action of amiloride on a Na^+ channel in toad urinary bladder by the transition of the molecule into such a lazy state (Lindemann, 1986*a*,*b*). Armstrong and Bezanilla (1977) concluded the existence of several closed states of the Na^+ channel in nerve cells from the temporal behavior of gating currents.

In this paper it is shown that a distinction between the different models of transport control can be based on the study of the behavior of steady-state current-voltage relationships (*I/V* curves). According to the findings of Fisahn and Hansen (1986) and of Fisahn et al. (1986*b*), there are two transporters in *Nitella* which can be considered for such an analysis, the H^+ pump and the K^+ channel. The H^+ pump in our cells has a reversal potential of about −450 mV, as concluded from the high impedance (Fisahn et al., 1986*b*, Fisahn & Hansen, 1986) and from unpublished *I/V* curve measurements. This is in line with findings of Beilby (1984) and Lucas (1982) who assigned a stoichiometry of 1 H^+/ATP to the H^+ pump in *Chara*, and in contrast to the findings of Kishimoto et al. (1984), who came to the conclusion that the stoichiometry is 2. Thus, only a small part of the pump *I/V* curve is accessible in the "voltage-window" from −450 to +200 mV.

The situation is more favorable in the case of the K^+ transporter. In a previous paper (Fisahn, Hansen & Gradmann, 1986) it was shown that the K^+ transporter in *Nitella* can be described by a Class-I model (Hansen et al., 1981). This finding was a surprise to us, as we believed that the Class-I mechanisms were restricted to electrogenic pumps and to cotransporters. However, prior to that investigation, Gradmann, Klieber and Hansen (1987) realized that *I/V* curves of a single K^+ channel from patch-clamp experiments on protoplasts of *Vicia faba* (Schroeder, Hedrich & Fernandez, 1984) could be described by the Class-I model. In addition, saturation regions of the *I/V* curves of a K^+ transporter indicating the involvement of cyclic Class-I transporters were found in patch-clamp studies of protoplasmic droplets of *Chara* (Lühring, 1986) and of *Acetabularia* (Bertl & Gradmann, 1986). The major part of the *I/V* curves of this transporter is in the accessible voltage window.

These findings encouraged us to make use of the temperature effect for the study of the mechanism controlling the activity of a transporter. A theory on which such an analysis can be based was published by Hansen et al. (1983). In order to explain peculiarities of the electrical impedance of biological membranes, two models were proposed. One of them, the so-called Class-I model B, the lazy-state model, deals with the activation and deactivation of membrane transport by the exchange of the transport cycle with an inactive (lazy) state *L*.

Materials and Methods

The setup and the experimental procedures are similar to those described in previous papers (Fisahn & Hansen, 1986; Fisahn et al., 1986*a*,*b*). Briefly, *Nitella flexilis* was purchased from R. Kiel in Frankfurt and kept in APW (0.1 mol m^{-3} KCl, 1.0 mol m^{-3} NaCl, 0.5 mol m^{-3} $CaCl_2$, no buffer) in a refrigerator at 10°C at a light intensity of 5 W m^{-2} (16 hr · d^{-1}). pH was adjusted by small amounts of HCl, when the pH-meter showed deviations of 0.5 pH units. Experiments were performed in 10 mol m^{-3} KCl, because Fisahn et al. (1986*a*) have shown that under these conditions the K^+ transporter with saturating *I/V* curves dominates the electrical characteristics of the membrane.

I/V-curve runs in the dark at high outside KCl, as necessary for bringing the cell in a state which shows the original *I/V* curves of the channel (*see* Discussion below) provide a serious stress for the cells (Beilby, 1986*a*; Fisahn et al., 1986*a*). As long lifetimes are required for a series of experiments at different temperatures, cells of good health were required. Thus, point-clamp of intact cells was applied. Short cells (2 cm length with a diameter of 0.5 mm) were selected in order to keep the cable problems small.

The cable problems could have been avoided by using single membrane samples (Hirono & Mitsui, 1983; Beilby & Blatt, *in preparation*), or air gaps (Sokolik & Yurin, 1986), or a central current electrode (Beilby, 1984). However, these techniques might have increased the health problem. We regarded the cable problem to be less serious because of three reasons. 1. The *I/V* curves with saturation regions are less sensitive to the cable problem, because in the saturation region, the current does not depend on the membrane potential. Consequently, the value of the current at the ends of the cell is not influenced by the longitudinal decay of the membrane potential. 2. The cable problems cannot perturbate the symmetry of the temperature effect on the *I/V* curves which is the crucial feature for the statement obtained in this paper. 3. V. Delfs in our laboratory installed the cable-correction program suggested by Smith (1984) on a personal computer. The calculations based on a longitudinal resistance of 10 MΩ/m showed that the "real" current was higher than the input current by about 15% in the experiments at 25°C and by about 7% in those at 5°C. The curve shapes did not change. The results of these calculations verified that the two features mentioned above prevented changes in the basic behavior of the curves.

The setup for temperature regulation is described by Fisahn and Hansen (1986). The bathing medium (10 mol m^{-3}) flowed through a cooler and then through a heater which set the temperatures to a desired value between 5 and 25°C. Light intensity was zero in the temperature experiments.

I/V curves (current-voltage relationships) were measured under voltage clamp. Two electrodes were inserted into the middle of the cell. By means of a relay in the tip of the preamplifiers the electrode could be connected to the FET-OP 3140 (RCA) for the measurement of membrane potential, or via 10 kΩ to the output of the clamp amplifier for current injection during the

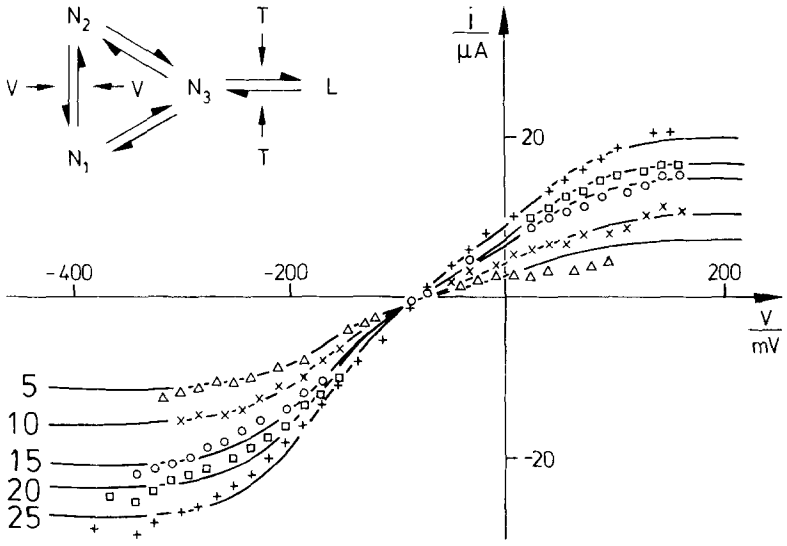

Fig. 1. Set of current-voltage curves obtained from *Nitella* at different temperatures. The numbers attached to the curves give the temperatures in °C. The currents are input currents of the whole cell, length 2 cm, diameter 0.5 mm, no light. The curves were subject to curve fitting on the basis of the lazy-state model in Fig. 2*B* by means of Eq. (5b). The model of Eq. (5b) used for fitting these curves is given in the inset. The parameters of Eq. (5b) are as follows: $zFN_t = 1$, $k^0_{io} = 207$, $k^0_{oi} = 633$, $\kappa_{io} = 403$, $\kappa_{oi} = 5790$, $m = 25.6$ common to all data sets, and $xm = 336, 242, 176, 155, 131$ for the temperatures 5, 10, 15, 10, 25°C, respectively

measurement of an *I/V* curve. It became necessary to change the solution in the current electrode from normally 1000 mol m^{-3} KCl to 3000 mol m^{-3} KCl plus 100 mol m^{-3} $AlCl_3$ in order to supply enough current to the cell. The clamp amplifier was homemade with a high-voltage OP (Burr Brown 3584 JM) supplying pulses up to +/−110 V, and resulting in a settling time of the membrane potential of 2 msec.

For the measurement of the *I/V* curves under voltage clamp, a series of alternating increasing pulses (120 + 80 + 120 + 80 msec for a subunit comprising resting potential, hyperpolarizing step, resting potential, depolarizing step) was used as in the previous investigation (Fisahn et al., 1986*a*), in order to reduce the stimulating action on excitation processes and the development of negative resistance (Beilby, 1986*a,b*) which takes about 100 msec (Hansen, 1986). The display of the current pulses on an oscilloscope was used to check for the absence of interference from effects of this kind. At outside K^+ concentrations higher than 1 mol m^{-3}, the current returned within 2 msec to a steady level. An Apple II microcomputer took care of the generation of the bipolar stair-case voltage command signal and of the data acquisition. The computer stored the average of the current and of the potential during the last 10 msec of each of the steps mentioned above. For curve fitting of the *I/V* curves, the program PUMA.ALG was used, which is an improved version of PUMO.FOR generated in 1979 in the laboratory of C.L. Slayman, New Haven, Connecticut.

Nomenclature: N_o and N_i are used for the two states of the pseudo-2-state model (Fig. 2*A*) of the active cycle. They include N_3, but exclude *L*. N_1 and N_2 are used for the 3-state model of the active cycle (Fig. 2*B*) excluding *L*. N_1 and N_2 do not include N_3. The same convention holds for the reserve factors r_1, r_2, r_i, r_o.

Results

The Curve-shape of the Measured *I/V* Curves: The Application of the Class-I Model to a K^+ Channel

Figure 1 displays a set of *I/V* curves taken at different temperatures, measured at an outside concentration of 10 mol m^{-3} KCl. At this concentration, the saturable K^+ transporter dominates the electrical properties of *Nitella*, and little interference from other transporters has to be taken into account (Fisahn et al., 1968*a*). Again, we found that the cells could stand positive potentials up to +200 mV, and that there was little interference from action potentials and negative resistance (Beilby, 1986*a,b*). As mentioned in the previous paper (Fisahn et al., 1986*a*), we added 0.2 mol m^{-3} $LaCl_3$ to the bathing medium in our first experiments in order to prevent action potentials (Beilby, 1984), but later it was omitted because interference from action potentials was rare, even though the cells were excitable.

In Fig. 1. the symbols give the experimental data and the smooth lines are obtained by the curve-fitting procedures described below. These curves display the saturation of current at positive and at negative potentials. These curve shapes are similar to those obtained in patch-clamp experiments of the K^+ channel (Schroeder et al., 1984; Bertl & Gradmann, 1986; Lühring, 1986). Gradmann et al. (1987) showed that the curve shape resulted from a cyclic transporter model and not from a diffusion-limited channel. The observation and evaluation of these *I/V* curves in *Nitella* was described by Fisahn et al. (1986*a*).

Even though Läuger (1980) came to the conclusion that "a unified description of ion carriers, channels, and pumps seems possible," we ourselves were surprised that the Class I model, originally developed for pumps (Hansen et al., 1981), can be applied to K^+ channels in plant cells, too (Fisahn et al., 1986*a*; Gradmann et al., 1987). Thus, the reliability of these results is discussed before we proceed with its application.

The occurrence of the *I/V* curves with the satu-

ration regions as shown in Fig. 1 is a peculiarity. A great variety of other curve shapes is shown by other authors. Especially at low $[K^+]_o$, the *I/V* curves display an increase of current at positive and at negative potentials, similar to the *I/V* curves of single or of pairs of anti-parallel semiconductor diodes. These *I/V* curves can be observed in *Nitella* (Sokolik & Yurin, 1981, 1986), in *Chara* (Coleman & Findlay, 1985; Beilby, 1986*a,b*) or in *Eremosphaera* (Köhler et al., 1986). Sokolik and Yurin (1981, 1986) found that the shape of the *I/V* curves depended on a so-called conditioning voltage, which was applied to the cell prior to the run of the *I/V* curve measurement. They assumed that different potassium channels, namely *D* channels and *H* channels, can be found in *Nitella*. The *D* channels, induced by a depolarizing conditioning voltage, displayed saturation at potentials more negative than ca. −150 mV in some experiments, whereas the range of positive potentials was not shown. Beilby (1985), too, interpreted her findings in *Chara* by the assumption of two different channels. In the first series of experiments, she distinguished between an unspecific "leak" and K^+ channel. In a later paper (Beilby, 1986*b*), she found K^+ sensitivity of the leak, too. At negative potentials, the downward bending can result from another hazard: Coster and Hope (1968) and Tyerman, Findlay and Paterson (1986*a,b*) reported an increase of chloride fluxes at negative potentials.

The curve shape shown in Fig. 1 is observed in intact cells very rarely. Beilby (1985) showed such a curve in cells presoaked in 2 and 5 mol m^{-3} Na^+, but she attributes this curve to the proton pump which was more active in her *Chara* than in our *Nitella*. Other regions of saturating current found in *I/V* curves of *Chara* at potentials more negative than −300 mV or more positive than −50 mV were also assigned to the H^+ pump (Beilby 1984; Kishimoto et al., 1984).

In contrast to the results from intact cells, patch-clamp experiments on K^+ channels in *Vicia faba* (Schroeder et al., 1984; Gradmann et al., 1987), in *Chara* (Lühring, 1986) or in *Acetabularia* (Bertl & Gradmann, 1986) revealed *I/V* curves with saturation regions like those in Fig. 1, as mentioned above.

Probably, the experiments of Bertl and Gradmann (1986) can provide the key for the understanding of the different *I/V* curves. The saturation curves, similar to those in Fig. 1, are found if the current of the open channel is plotted versus membrane potential. If the average current (including open and closed states) is taken, then *I/V* curves are found which show an increase of current at depolarized potentials.

The experiments of Bertl and Gradmann (1986) lead to the conclusion that the basic curve shape of the *I/V* curve of the K^+ channel is of the saturating type shown in Fig. 1. The deviations commonly observed in intact cells are introduced by the activation-deactivation properties of the channel, since measuring the current of an intact cell implies averaging over many channels in different states.

Bertl and Gradmann (1986) explained this behavior by a model with two "lazy states" (Hansen et al., 1983) of the transport molecule. One of them L_i performs the exchange with the transport cycle via voltage-insensitive rate-constants; the other one L_v via voltage-sensitive rate constants. It is the voltage-sensitive exchange with L_v which causes the deviations from the saturating *I/V* curves. Lazy states with voltage-insensitive rate constants cannot change the basic shape of a Class I *I/V* curve (Hansen et al., 1981, 1983).

Beilby (*personal communication*) raised the following argument against our results: Cable problems originating from the applied point clamp might smooth out the region of negative impedance (Ohkawa & Kishimoto, 1977; Coleman & Findlay, 1985; Beilby, 1986*b*; Hansen, 1986; Köhler et al., 1986; Sokolik & Yurin, 1986;), thus pretending the occurrence of saturation. The following features convinced us that this does not occur.

1. We observed the region of negative resistance in many other experiments, mainly in *Chara* (Hansen, 1986). Thus, we know that our recording technique reveals the negative slopes if they occur.

2. In experiments making use of Ogata's water film electrode (Ogata, 1983) the negative slopes occurred in about 10% of all records. This shows that also in experiments in which the cable problem was eliminated negative slopes occurred rarely (in our cells in contrast to those of Beilby).

3. The negative slope develops with time (Coleman & Findlay, 1985; Hansen, 1986). Consequent upon this, all records of the time-course of the current pulses in those *I/V*-curve studies which reveal negative slopes display a strong variation of the current with time (Beilby, 1985; Coleman & Findlay, 1985; Sokolik & Yurin, 1986).

In our experiments, the time-course of the current steps did not exhibit these transients. The analysis of the time-courses (*unpublished results* of V. Delfs) showed that the component, originating from the loading of the membrane capacitor via the cell wall resistance and via internal cable resistances (time constant about 2 msec) was independent on membrane potential indicating the absence of unstirred layer effects and little influence of membrane potential on the cable properties. The second component (time constant 10 to 100 msec) shows that

exchange with the lazy states is small, probably restricted to the exchange with the voltage-insensitive lazy state (*see* Discussion).

The occurrence of negative slopes requires the involvement of a Class II model (two pairs of rate-constants being sensitive to membrane potential) as provided by the incorporation of a lazy state with voltage-sensitive rate constants (Gradmann, 1984; Bertl & Gradmann, 1986; Hansen, 1986). Thus, the occurrence of negative slopes depends on the magnitude of the exchange of the active states with this lazy state. The recent paper of Fisahn and Hansen (1986) and the investigations in this article show that the lazy states play a vital role in the control of transport by signals from other functional units in the cells. Thus, depending on these signals, the coupling of the lazy states to the transport cycle can be more or less tight. This model explains that in different cultures a great variety of curve shapes can occur. We were lucky (for the purpose of this and the preceding paper, Fisahn et al., 1986*a*) that in our cells grown at low-light intensity and at 10°C, which lived at low resting potentials (about −120 mV), the exchange of the active cycle with the voltage-sensitive lazy state was very small. This results in three phenomena which should occur together:

1. The "original I/V curves of the channel," namely the saturating I/V curves become visible.
2. No negative slopes.
3. Simple temporal behavior of the clamp current induced by the steps in potential.

In this model, the role of the conditioning voltage applied by Sokolik and Yurin (1981, 1986) is understood. It sets the exchange parameters with the voltage-sensitive lazy state. Additional support for such a view is obtained by measurements of the voltage dependence of the components of the low-frequency noise of membrane potential in *Nitella*. The noise studies reveal different modes of coupling of metabolic noise to the transport molecule depending on the dominant type of the I/V curve (*unpublished results* of R. Willkomm in our laboratory).

The Influence of Temperature

As indicated in Fig. 1, temperature was changed in steps of 5°C from 5 to 25°C. After each temperature step, the cell was given 5 to 10 min to adjust to the new temperature. This time is expected to be long enough as the time constant of the action of temperature on membrane resistance was found to be about 40 sec (Fisahn & Hansen, 1986). It should be mentioned that this effect of temperature on the I/V curves is not caused by a direct action of temperature on the transport molecule, but mediated by a signal from another functional unit in the cell (Fisahn & Hansen, 1986), which is the photosynthetic apparatus according to unpublished findings of Susanne Stein in our laboratory.

In contrast to the influence of outside K^+ studied in the preceding paper (Fisahn et al., 1986*a*), the changes in temperature result in changes of the positive saturation currents as well as of the negative saturation currents, as shown in Fig. 1.

Curve Fitting

Curve fitting of the I/V curves of this K^+ transporter is already described in the previous paper (Fisahn et al., 1986*a*). The analysis was based on the Class I models shown in Fig. 2. The theory of Class I models is given by Hansen et al. (1981). Class I comprises all models with one pair (being the reason for the name Class I) of reaction constants being sensitive to membrane potential. By convention, these two rate constants are k_{12} and k_{21} located between state 1 and state 2. A "real" reaction scheme with n states can be represented by a model with less states along the following rules:

1. All reactions which are not influenced by the actual experimental treatment may be lumped into the neutral recycling reactions.
2. Those reaction constants which are attacked by the experimenter must not be lumped into overall reactions.
3. The experimenter has to realize that the reaction constants obtained from the analysis include unknown reserve factors. This holds for every kind of kinetic analysis.

Thus, the genuine model for the description of a single Class-I I/V curve is the 2-state model (Hansen et al., 1981), because only the electrosensitive reactions k_{io} and k_{oi} have to be excluded from the lumped recycling reactions κ_{io} and κ_{oi} (Fig. 2*A*).

In the experiments of the previous paper (Fisahn et al., 1986*a*), the change of substrate concentration demands the additional reaction pair of the 3-state model shown in Figs. 2(*C*) and 2(*E*). From that analysis, the charge of the naked transporter ($z = 0$), and the stoichiometry (1 K^+ per cycle) was obtained. It was found that the reaction constant of binding outside K^+ increased linearly with $[K^+]_0$.

In this paper, the effect of temperature is investigated. At the beginning of the analysis, we did not know which reaction of the transport cycle is changed by the action of the involved control loop. Different mechanisms can be visualized, which can be assigned to two groups. In one group, reactions within the cycle are modified (Figs. 2*C* to *E*) for

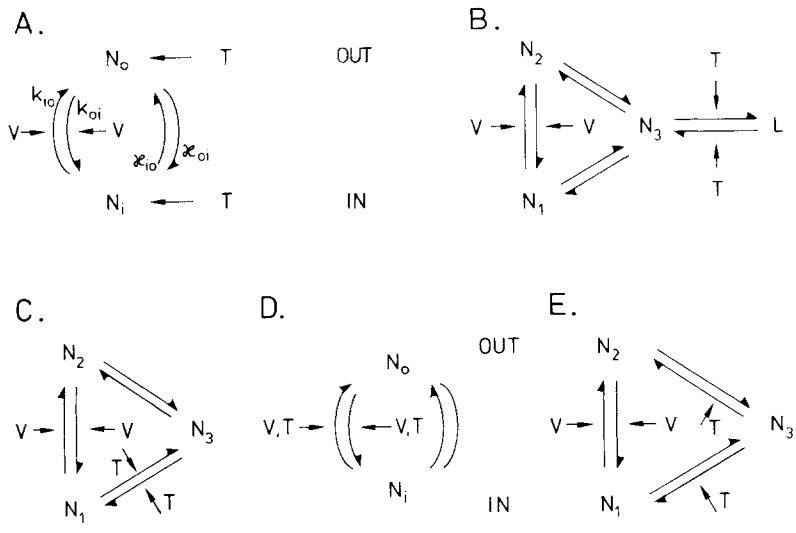

Fig. 2. Different models considered for the fitting of the curves in Fig. 1. (*A* and *B*) inactivation and deactivation of transporters: (*A*) Unspecific change in transporter number. (*B*) Lazy-state model, exchange of the cycle with an inactive state. (*C*, *D* and *E*) Catalytic effects, decrease in transport activity by slowing down of reaction rates: (*C*) Increase of an energy barrier between states 1 and 3. (*D*) Increase of an energy barrier between state 1 and state 2. (*E*) Changes in the stability of a state. Fits based on model *B* are shown in Fig. 1; fits based on model *D* are displayed in Fig. 3

instance by changing the height of an energy barrier or by changing the decay rate of the state in the cycle. These catalytic reactions make two rate constants of opposite direction change by the same factor. Otherwise, the reversal potential would be influenced. In the other group, transporters are deactivated. This deactivation may be assumed to change the number of active transporters N_t which is independent of the actual state of the transport molecule, or to cause an exchange of the active cycle with a lazy-state L (Fig. 2*B*).

The different models can be described by the 2-state or by the 3-state current-voltage relationships, which are

$$i = \frac{zF\,N_t\,(k_{io}\,\kappa_{oi} - k_{oi}\,\kappa_{io})}{k_{io} + k_{oi} + \kappa_{io} + \kappa_{oi}} \tag{1}$$

for the 2-state model and

$$i = \frac{z\,F\,N_t\,(k_{12}k_{23}k_{31} - k_{21}k_{32}k_{13})}{k_{12}(k_{23} + k_{32} + k_{31}) + k_{21}(k_{13} + k_{32} + k_{31}) + k_{13}(k_{23} + k_{32}) + k_{31}k_{23}} \tag{2}$$

for the 3-state model (Hansen et al.,1981). z and F have their usual meanings, N_t = total amount of transporters. The voltage-dependence is introduced by the voltage sensitivity of k_{12} and k_{21} (or k_{io} and k_{oi} in a similar way) according to the assumption of a symmetrical energy barrier (Läuger & Stark, 1970; Hansen et al., 1981). This assumption is reasonable because a different location of the energy barrier leads to asymmetric curve shapes, which are clearly different from those in Fig. 1, as can be shown by model calculations (Gradmann et al., 1987).

$$k_{12} = k_{12}^0 \exp(zFV/RT) \tag{3a}$$

$$k_{21} = k_{21}^0 \exp(-zFV/RT). \tag{3b}$$

The action of the control loop is introduced by making one or two reaction constants dependent on x:

$$k_{ij} = k_{ij}^0\,x \tag{4}$$

with x describing the action of the control loop on the transporter (here: temperature effect).

From previous investigations (Fisahn et al., 1986; Fisahn & Hansen, 1986) we know that there is still a residual activity of another transporter, which acts as a current source (pump or cotransporter), whose activity, too, is influenced by temperature, as mentioned in the Introduction. Thus, a voltage-independent term P is included in the equations used for curve fitting. This term has to be introduced also because of another reason: The investigations mentioned above show that temperature acts via control signals which should not contribute to the energy balance of the transporter. Thus, they cannot change the reversal potential. The only source for changes of the reversal potential is the factor RT/F (which is 0.5 mV/°C) and the involvement of another transporter. Curve fitting will show whether this degree of freedom is necessary, because it does not interfere with the other degrees of freedom, which cannot change the reversal potential.

In Fig. 2, different models of a possible action of the temperature-stimulated control loop on the K^+ transporter are shown. These models differ by the reactions which are assumed to be influenced by the controller. These assumptions lead to different locations of x (Eq. 4) in the following equations:

Fig. 2(A)

Change in the number of transporters. A 2-state model is required in which N_t is changed by temperature:

$$i = \frac{zFxN_t(k_{io}\kappa_{oi} - k_{oi}\kappa_{io})}{k_{io} + k_{oi} + \kappa_{io} + \kappa_{oi}} + P. \quad (5a)$$

Fig. 2(B)

Exchange with the lazy state. The resulting equation is derived in the Appendix (Eq. A19).

$$i = \frac{zFN_t(k_{io}\kappa_{oi} - k_{oi}\kappa_{io})}{(1 + xm)(k_{io} + \kappa_{io}) + (1 + x)(k_{oi} + \kappa_{oi})} + P. \quad (5b)$$

Fig. 2(C)

Effect on a neutral reaction pair, e.g. k_{31} and k_{13}. This may be achieved by a change in the height of an energy barrier. A 3-state model is required since the effects of potential and of temperature occur at different places.

$$i = \frac{zFN_tx(k_{12}k_{23}k_{31}^0 - k_{21}k_{32}k_{13}^0}{k_{12}(k_{23} + k_{32} + xk_{31}^0) + k_{21}(xk_{13}^0 + k_{32} + xk_{31}^0) + xk_{13}^0(k_{23} + k_{32}) + xk_{31}^0k_{23}} + P. \quad (5c)$$

Fig. 2(D)

Effect on the pair of electrosensitive reaction constants. Again, the height of an energy barrier is changed. In this case a 2-state model can be used, because the same reaction pair is influenced by voltage and temperature. The related equation is:

$$i = \frac{zFN_t(k_{io}x\kappa_{oi} - k_{oi}x\kappa_{io})}{x(k_{io} + k_{oi}) + \kappa_{io} + \kappa_{oi}} + P. \quad (5d)$$

Fig. 2(E)

Catalytic effect, the stability of a complex is changed, and the decay reaction to either side has changed, e.g. k_{32} and k_{31}. A 3-state model is required

$$i = \frac{zFN_tx(k_{12}k_{23}k_{31}^0 - k_{21}k_{32}^0k_{13})}{k_{12}(k_{23} + xk_{32}^0 + xk_{31}^0) + k_{21}(k_{13} + xk_{32}^0 + xk_{31}^0) + k_{13}(k_{23} + xk_{32}^0) + xk_{31}^0k_{23}} + P. \quad (5e)$$

The applicability of the models shown in Fig. 2 was tested by subjecting the data to a joint-fit analysis. In the curve-fitting routines, x and P in the equations above were allowed to be different for the individual data sets obtained at different temperatures, whereas the same set of k reaction rates had to be used for all data sets.

In Fig. 1, a fit based on the lazy-state model (Fig. 2*B*) is shown. Figure 1 shows that the curves calculated by the computer are very close to the experimental data points. Deviations are seen for the 5°C curve at positive potentials and for the 25°C curve at negative potentials. We think that 5°C is already pretty cold and secondary effects of the temperature may be involved. The deviation may also result from an interference from incomplete suppression of the negative resistance region described by Beilby (1986*b*) which we hoped to suppress by the alternating pulse series and/or $LaCl_3$. The downward bending at negative potentials probably results from the involvement of an additional transporter, presumably a chloride channel, which opens at very negative potentials (Coster & Hope, 1968; Tyerman et al., 1986*a*,*b*) as discussed in our previous paper (Fisahn et al., 1986*a*).

The lazy-state model applied in Fig. 1 gave the best fit. A good fit is also obtained by the model of Fig. 2(*A*), assuming a change in transporter number (N_t). This fit does not differ very much from that shown in Fig. 1, and thus it is not displayed here. A very bad fit (Fig. 3) is obtained, when a change of the electrosensitive reactions is assumed (model in Fig. 2*D*). Bad fits are also obtained by the other models assuming a catalytic mode of action of the control mechanism (Figs. 2*C* and *E*). A closer inspection of the error sums is given below.

In Table 1, the numerical data are given which are obtained from the curve fitting on the basis of the best model (Fig. 1 and Fig. 2*B*).

The location of N_3 and thus of L is given by m (Eq. A22a in the Appendix).

$$m = r_{o3}/r_{i3}. \quad (6)$$

The value of m of 37 in Table 1 implies that the lazy state is closely related to N_2, the outside representative state. This does not imply a physical location at the outer side of the membrane, but faster rate constants from N_2 to N_3 than from N_1. This kinetic location of N_3 is in line with previous measurements of the membrane impedance showing inductive behavior at hyperpolarizing potentials

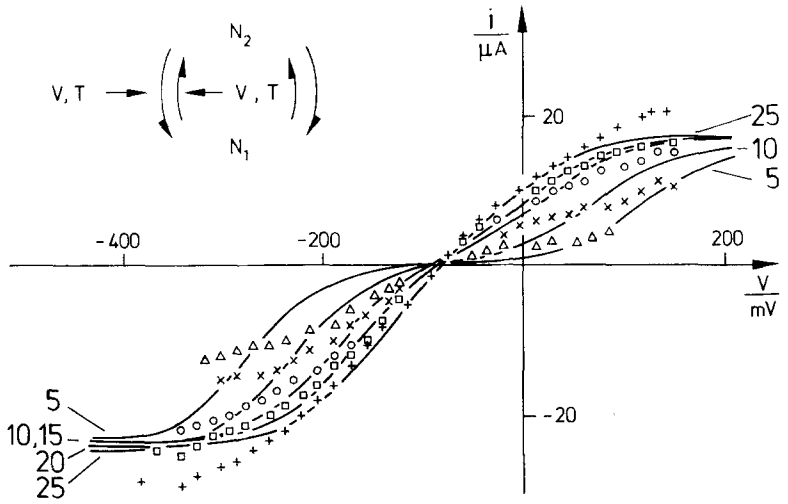

Fig. 3. The "best" fit based on model *D* of Fig. 2. The same data as in Fig. 1 are fitted by Eq. (5d). Model *D* assumes that temperature changes the Eyring barrier across which the charged complex has to hop

Table 1. Temperature effect[a]

	k_{io}^0	k_{oi}^0	κ_{io}	κ_{oi}	m
Value	175	540	277	3215	37
Scatter	1.3	1.5	1.5	2.1	1.8
T°C	5	10	15	20	25
$x\,m$	218	163	122	109	88
x	5.9	4.4	3.3	2.9	2.4
Scatter	1.5	1.4	1.4	1.3	1.4
P	0.001	0.018	0.122	0.127	0.252
Scatter	1.1	4.0	1.7	1.4	1.6

[a] Upper part: The constraint (common to all data sets) 2-state reaction constants of the lazy-state model in Fig. 2*B* (dimension is sec^{-1} for $zFN_t = 1$) obtained from curve fitting of five data sets by Eq. (5b). Lower part: Dependence of the free parameters x and P on temperature. The scatter is given as a factor according to averaging in a logarithmic scale.

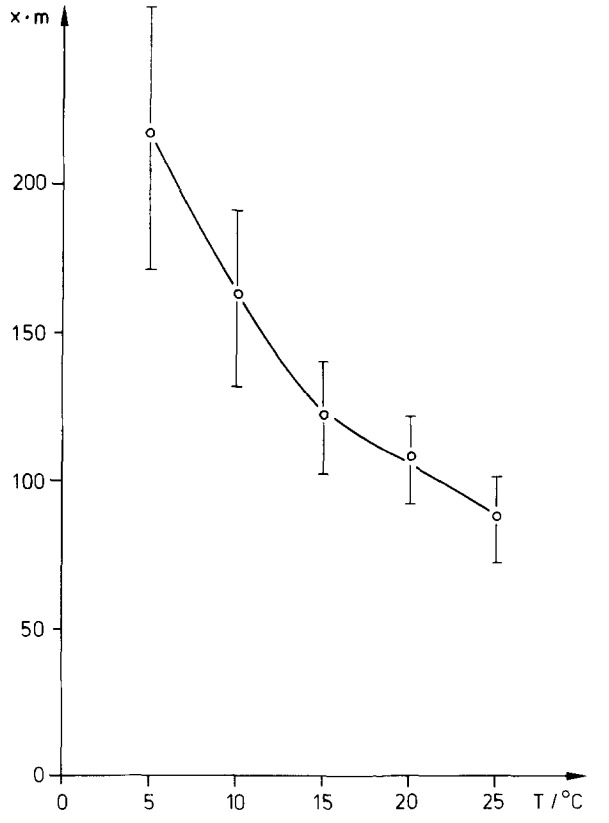

Fig. 4. Dependence of xm (Eq. 5b) on temperature. Data from Table 1

(Hansen et al., 1983; Hansen, 1986). Unpublished studies of R. Willkomm in our laboratory have shown that the inductive behavior is found only in those cells which display the saturating I/V curves, whereas a capacitive component peaks at E_K, if the nonsaturating I/V curves occur.

The lower part of Table 1 displays the dependence of x on temperature. As shown in the Appendix, x is related to the ratio of forward and backward reaction in the exchange between the lazy-state L and the transport cycle as given by Eq. (A22). By means of Eq. (A21), Eq. (A22) can be converted to an alternative form

$$xm = k_{3L}/k_{L3}\, r_{o3}. \tag{7}$$

The involvement of r_{o3} (Eq. A20f) renders the calculation of the ratio k_{3L}/k_{L3} from xm difficult. However, the dependence of this ratio on temperature is seen from Fig. 4, as r_{o3} is assumed to stay constant. It is seen that the transporters come out of L with increasing temperature.

The relationship between the states in the cycle and in L is given by Eq. (A25).

Table 2. The average error as calculated by Eq. (10) obtained from fitting five data sets by the five different models in Fig. 2[a]

Data set	A Transport number	B Lazy state	C k_{13} and k_{31}	D k_{12} and k_{21}	E k_{32} and k_{31}
1	0.31	0.25	0.31	0.40	0.59
2	0.31	0.29	0.41	0.78	0.71
3	0.28	0.27	0.40	0.78	0.62
4	0.40	0.33	0.50	1.60	0.56
5	0.38	0.35	0.47	0.80	0.62
Average	0.33	0.30	0.41	0.79	0.62
Scatter	1.1	1.1	1.2	1.6	1.1
t-var	1.4		3.59	3.2	12.1
Signif. Level	10%		0.5%	1%	0%

[a] In the last two rows, four of these models are compared with the lazy-state model (second column) by means of the student's *t*-test.

$$L = xN_i + xmN_o \tag{8}$$

with N_i and N_o being the apparent concentrations of the transporters at the inner and outer side (Eqs. A20g,h). As N_i and N_o change with membrane potential, L also changes with membrane potential. This is the cause of the changes in the shape of the I/V curves related to the action of L.

The values of xm, given in Table 1, are very high. The absolute values should not be taken very seriously. Equation (5b) shows that the value of about 200 of xm overrides the "1" in the denominator of Eq. (5b). Thus, a common factor may be extracted from $(1 + xm)$ and from $(1 + x)$ in Eq. (5b) and merged into N_t without major influence on the quality of the fit. Thus, the values of xm in Table 1 should not lead to the statement that the number of transporters in L is more than 200 times that in N_o. However, the dependence of xm on temperature is not influenced by this objection.

In Eq. (5b), the term P was used to account for a possible current source. It is found that P decreases rapidly with temperature. Even though we do not take the estimation of P very seriously, we should like to point out that P is strongly reduced at 5°C. This is in line with results of Gradmann (1970) who inhibited the Cl^- pump in *Acetabularia* by temperatures below 8°C.

The failure of the model D used for the fit in Fig. 3 is quite obvious. Thus, this model can be ruled out very clearly. The difference between the models in Fig. 2(A) and Fig. 2(B) was less striking. Thus the behavior of the error of the fits has to be investigated. Table 2 shows the error sums obtained from five data sets subject to fits by the five different models in Fig. 2. The error sum is calculated as follows

$$E = \sqrt{E^2} = \left\{ \frac{\sum_{i=1}^{NN} (i_m - i_t)^2}{NN - KK} \right\}^{1/2} \tag{10}$$

with NN being the number of all data points (5 times 32) and KK the number of degrees of freedom (7 or 9, depending on the model).

According to Table 2, preference is given to the lazy-state model as discussed below.

Discussion

In a preceeding investigation (Fisahn et al., 1986*a*) the analysis of the K^+ effect on the I/V curves in *Nitella* has shown that the K^+ channel is not yet a water-filled hole, but a more complicated mechanism. Transport by this channel is mediated by transitions between several states of the molecule, as assumed for the Na^+ channel in exitable membranes (Armstrong & Bezanilla, 1977). The important feature of the K^+ channel in *Nitella* is the recycling step, which is necessary to bring the molecule back into a state ready to accept a new passenger after the preceding one has been delivered. The existence of this recycling step leads to a kinetic behavior which can be described by the Class-I model originally developed for electrogenic pumps (Hansen et al., 1981). Further details of the application of this model to K^+ channels, e.g., the rejection of a diffusion-limited channel as an alternative explanation, are given by Gradmann et al. (1987).

Additional support for these findings comes from the patch-clamp experiments discussed above, and from the results of the investigations of this paper. The I/V curve analysis of the temperature effect on the K^+ transporter in *Nitella* has shown again that the curves can be analyzed by a Class-I model.

The peculiar question of the present investigations is whether this analysis is capable of revealing the locus at which the control unit interferes with the transport molecule. As mentioned in the Introduction, it has been shown in a preceeding paper (Fisahn & Hansen, 1986) that the main temperature effect is not due to a direct action on the transport molecule, but to secondary effects mediated via signals from the photosynthetic apparatus. The analysis of the changes of the steady-state I/V curves shows that some models can be ruled out, namely all those which start from the assumption that the

involved controller exerts a catalytic effect, i.e. changing the height of an energy barrier within the transport cycle. Other combinations which are not shown in Fig. 2 gave fits as bad as those of the model in Fig. 2(*E*), and are not discussed here in detail.

The 2-state Class-I model holds for the evaluation of a single *I/V* curve. If changes of the *I/V* curves with an experimental parameter are analyzed, additional degrees of freedom have to be introduced. This was one degree in the case of the effect of outside K^+ concentration (Fisahn et al., 1986*a*). In the case of the temperature effect investigated in this study, three additional degrees are introduced.

The following account of the degrees of freedom shows that the principle of a minimum extension of the model is not violated (number: description):

4: two-state variables for a single *I/V* curve

1: location of the energy-barrier is assumed to be in the middle of the membrane (Läuger & Stark, 1970). This is an arbitrary assumption. However, model calculations show that otherwise asymmetric *I/V* curves quite different from those in Fig. 1 are obtained (*see* discussion following Eq. 4). A more thorough discussion of this problem is given by Gradmann et al. (1987) showing that the data exclude any major influence of asymmetric or multi-peak energy barriers and of unstirred layers).

1: x for the temperature influence. A new variable (temperature) requires at least one new degree of freedom (theory of Class-I models, Hansen et al., 1981).

1: m for the asymmetric location of the lazy state L. As two alternative models (without and with m, model *A* and model *B*) are included, the computer can make the decision whether m is required or not.

1: P for a possible interference from a temperature influence on the pump as indicated by the preceding paper of Fisahn and Hansen (1986). As P causes a shift of the reversal potential which cannot be accomplished by x and m, P does not interfere with the determination of x and m. Thus, the computer can make the decision whether it is required or not.

The above account shows that the models considered in the curve-fitting routines are minimum models.

Two models give good fits, the lazy-state model and the assumption of an unspecific reduction of transporter number. The lazy-state model results in a slightly better fit. In either case, the conclusion holds that transport activity is controlled by activation and deactivation of transporters. Table 2 shows that the error sum obtains a minimum for the lazy-state model (Fig. 2*B*). However, the model in Fig. 2(*A*) also yields reasonable fits. In order to make a decision, a student's *t*-test is applied in Table 2. Table 2 shows that the hypothesis that the fits of model *A* and of model *B* are equal has a significance level of 10%. We leave the decision to the reader to judge about the significance. The difference between the two models is as follows: In model *B*, the (to our opinion only reasonable) mechanism of activation and deactivation is specified. In model *A*, activation and deactivation is independent of the state in which the transport molecule is. If state 3 were in the reaction kinetic middle between state i and state o ($k_{13} = k_{23}$ in Fig. 2(*B*), with $i = 1$ and $o = 2$), then there were no differences between the two models at all. The reason is that in that case N_3 would not change with the voltage-dependent occupation of N_1 and N_2. However, if N_3 were closer to N_2, a depletion of N_2 with negative potentials would lead to a depletion of N_3. As L is in equilibrium with N_3, transporters would come out of L back to work. The opposite effect happens at positive potentials or at negative potentials if N_3 were closer to N_1.

Consequent upon this, the state of inactivation is dependent on membrane potential. This leads to an additional inductive or capacitive time constant of the electrical impedance as described by Hansen et al. (1983).

The asymmetry of the location of N_3 is given by the parameter m in Eq. (5*B*). The high value of m in Table 1 implies that the lazy state is kinetically close to the outer state N_o. As mentioned above this does not mean that L is located at the outside of the membrane. However, it should be mentioned that the determination of m is that feature of the analysis which may suffer from the cable problem discussed in Materials and Methods.

Hansen et al. (1983) have predicted that under these conditions inductive behavior of the membrane impedance is expected if membrane potential is more hyperpolarized than the reversal potential E_K. This has been found by H.J. Martensen in our laboratory (*unpublished results* and Hansen, 1986). Additional support is given by the findings of Willkomm mentioned above.

Thanks are due to the Deutsche Forschungsgemeinschaft for financial support (Ha 712/7-3). We are grateful to Dr. M. Beilby, Sydney, for helpful discussions, to Mr. V. Delfs for calculating the cable influence according to the procedure of Smith (1984), to

Mrs. E. Götting for drawing the figures and to Mr. H. Mainzer for the construction of the clamp amplifier. Curve fitting was done on the PDP 10 of the Kieler Rechenzentrum.

References

Armstrong, C.M., Bezanilla, F. 1977. Inactivation of the sodium channel. II. Gating current experiments. *J. Gen. Physiol.* **70:**567–590

Beilby, M.J. 1984. Current-voltage characteristics of the proton pump at *Chara* plasmalemma: I. pH dependence. *J. Membrane Biol.* **81:**113–125.

Beilby, M.J. 1985. Potassium channels at *Chara* plasmalemma. *J. Exp. Bot.* **36:**228–239

Beilby, M.J. 1986*a*. Potassium channels and different states of *Chara* plasmalemma. *J. Membrane Biol.* **89:**241–249

Beilby, M.J. 1986*b*. Factors controlling the K^+-conductance in *Chara*. *J. Membrane Biol.* **93:**187–193

Bertl, A., Gradmann, D. 1986. Single-channel recordings from the plasmalemma of *Acetabularia*. *In:* 7th International Workshop on Plant Membrane Transport. Sydney (*in press*)

Coleman, H.A., Findlay, G.P. 1985. Ion channels in the membrane of *Chara inflata*. *J. Membrane Biol.* **83:**109–118

Coster, H.G.L., Hope, A.B. 1968. Ionic relations in cells of *Chara australis*. XI. Chloride fluxes. *Aust. J. Biol. Sci.* **21:**243–254

Fisahn, J., Hansen, U.P. 1986. The influence of temperature on a K^+-channel and on a current-source in *Nitella*. *J. Exp. Bot.* **37:**440–460

Fisahn, J., Hansen, U.P., Gradmann, D. 1986*a*. Determination of charge, stoichiometry and reaction-constants from *IV*-curve studies on a K^+-transporter in *Nitella*. *J. Membrane Biol.* **94:**245–252

Fisahn, J., Mikschl, E., Hansen, U.P. 1986*b*. Separate oscillations of a K^+-channel and of a current-source in *Nitella*. *J. Exp. Bot.* **37:**34–47

Gradmann, D. 1970. Einfluss von Licht, Temperatur, und Aussenmedium auf das elektrische Verhalten von *Acetabularia crenulata*. *Planta (Berlin)* **93:**323–553

Gradmann, D. 1984. Electrogenic Cl^--pump in the marine alga *Acetabularia*. *In:* Chloride Transport Coupling in Biological Membranes and Epithelia. G.A. Gerencser, editor. pp. 13–61. Elsevier, Amsterdam

Gradmann, D., Hansen, U.P., Slayman, C.L. 1982. Reaction kinetic analysis of current-voltage relationships for electrogenic pumps in *Neurospora* and *Acetabularia*. *In:* Electrogenic Ion Pumps. C.L. Slayman, editor. (*Current Topics in Membrane and Transport., Vol.* 16) pp. 257–276. Academic, New York

Gradmann, G., Klieber, H.G., Hansen, U.P. 1987. Reaction kinetic parameters for ion transport from steady-state current-voltage curves. *Biophys J.* **51:**569–585

Hansen, U.P. 1986. Reaction kinetic models of pumps, cotransporters and channels. *In*: Ion Channels and Electrogenic Pumps in Biomembranes. Abstracts of Lectures and Posters, Osaka University, pp. L13–L33

Hansen, U.P., Gradmann, D., Sanders, D., Slayman, C.L. 1981. Interpretation of current-voltage relationships for "active" ion transport systems: I. Steady-state reaction-kinetic analysis of class-I mechanisms. *J. Membrane Biol.* **63:**165–190

Hansen, U.P., Tittor, J., Gradmann, D. 1983. Interpretation of current-voltage relationships for "active" ion transport systems: II. Nonsteady-state reaction-kinetic analysis of Class-I mechanisms with one slow time-constant. *J. Membrane Biol.* **75:**141–169

Hirono, C., Mitsui, T. 1983. Slow onset of activation and delay of inactivation in transient current of *Nitella axilliformis*. *Plant Cell Physiol.* **24:**289–299

Kishimoto, U., Kami-ike, N., Takeuchi, Y., Ohkawa, T. 1984. A kinetic analysis of the electrogenic pump of *Chara corallina*. I. Inhibition of the pump by DCCD. *J. Membrane Biol.* **80:**175–183

Köhler, K., Steigner, W., Kolbowski, J., Hansen, U.P., Simonis, W., Urbach, W. 1986. Potassium channels in *Eremosphaera viridis*. II. Current- and voltage-clamp experiments. *Planta* **167:**66–75

Läuger, P. 1980. Kinetic properties of ion carriers and channels. *J. Membrane Biol.* **57:**163–178

Läuger, P., Stark, G. 1970. Kinetics of carrier-mediated transport across lipid bilayer membranes. *Biochim. Biophys. Acta* **211:**458–466

Lindemann, B. 1986*a*. Blocking kinetics of Na channels in apical membranes. *In:* Proc. Int. Union Physiol. Sci., Vol. XVI, p. 343

Lindemann, B. 1986*b*. Die Natrium-Kanäle der Epithelien: Transportkinetik, Blockierungskinetik und Regulation. *In:* Physiologie Aktuell. B. Bromm and D.W. Lübbers, editors. Vol. 2, pp. 111–125. Fischer, Stuttgart, New York

Lucas, W.J. 1982. How are the plasmalemma transport processes of *Chara* regulated? *In:* Membrane Transport in Plants. W.J. Cram, K. Janacek, R. Rybova and K. Sigler, editors. pp. 459–466. Akademia, Prague

Lühring, H. 1986. Recording of single K^+ channels in the membrane of cytoplasmic drop of *Chara australis*. *Protoplasma* **133:**19–28

Ogata, K. 1983. The water-film electrode: A new device for measuring the *characean* electropotential and conductance distributions along the length of the internode. *Plant Cell Physiol.* **24:**695–703

Ohkawa, T., Kishimoto, U. 1977. Breakdown phenomena in the *Chara* membrane. *Plant Cell Physiol.* **17:**201–207

Schroeder, J.I., Hedrich, R., Fernandez, J.M. 1984. Potassium selective single channels in guard cell protoplasts of *Vicia faba*. *Nature (London)* **312:**361–362

Smith, J.R. 1984. The electrical properties of plant cell membranes. II. Distorsion of non-linear current-voltage characteristics induced by the cable properties of *Chara*. *Aust. J. Plant Physiol.* **11:**211–224

Sokolik, A.I., Yurin, V.M. 1981. Transport properties of potassium channels of the plasmalemma in *Nitella* cells at rest. *Soviet Plant Physiol.* **28:**206–212

Sokolik, A.I., Yurin, V.M. 1986. Potassium channels in plasmalemma of *Nitella* cells at rest. *J. Membrane Biol.* **89:**9–22

Tyerman, S.D., Findlay, G.P., Paterson, G.J. 1986*a*. Inward membrane current in *Chara inflata*. I. A voltage- and time-dependent Cl^- component. *J. Membrane Biol.* **89:**139–152

Tyerman, S.D., Findlay, G.P., Paterson, G.J. 1986*b*. Inward membrane current in *Chara inflata*. II. Effects of pH, Cl^--channel blockers and NH_4^+, and significance for the hyperpolarized state. *J. Membrane Biol.* **89:**153–161

Warncke, J., Lindemann, B. 1985. Voltage-dependence of Na channel blockage by amiloride: Relaxation effects in admittance spectra. *J. Membrane Biol.* **86:**255–265

Received 3 September 1986; revised 16 March 1987

Appendix

Calculation of the effect of the occupation of a lazy-state L on the steady-state I/V curves of a Class-I model

A. Rate Equations

The pseudo-4-state model in Fig. 2(*B*) leads to the following set of rate equations ("κ" describes gross rate constants)

$$\frac{dN_1}{dt} = k_{21}N_2 + \kappa_{31}N_3 - (k_{12} + \kappa_{13})N_1 \tag{A1}$$

$$\frac{dN_2}{dt} = k_{12}N_1 + \kappa_{32}N_3 - (k_{21} + \kappa_{23})N_2 \tag{A2}$$

$$\frac{dN_3}{dt} = \kappa_{13}N_1 + \kappa_{23}N_2 + k_{L3}L - (\kappa_{31} + \kappa_{32} + k_{3L})N_3 \tag{A3}$$

$$\frac{dL}{dt} = k_{3L}N_3 - k_{L3}L. \tag{A4}$$

B. Calculation of Steady-State Membrane Current

The calculation of steady-state transport activity is based on the premises that all d/dt are zero. In case of Eq. (A4) this leads to

$$L = \frac{k_{3L}}{k_{L3}} N_3 = qN_3. \tag{A5}$$

Inserting Eq. (A5) into Eq. (A3) results in

$$\frac{dN_3}{dt} = \kappa_{13}N_1 + \kappa_{23}N_2 - (\kappa_{31} + \kappa_{32})N_3. \tag{A6}$$

Thus, the lazy-state L does not show up in the calculation of the equilibrium relationships. However, this does not mean that L does not show up at all. For the calculation of the current mediated by the transport system, the law of conservation of carriers has to be incorporated, and that requires the summation over all states in which the carriers can occur (Eqs. A11a,b).

The current can be calculated from the following equation (Fig. 2):

$$I = zF(N_1k_{12} - N_2k_{21}) \tag{A7}$$

as the transitions between N_1 and N_2 are the only ones which translocate charge in a Class-I model. Voltage-sensitivity enters the equation via

$$k_{12} = k_{12}^0 \exp(V/2u_T),\ k_{21} = k_{21}^0 \exp(-V/2u_T). \tag{A8a,b}$$

The exponent comprising the temperature potential u_T

$$u_T = RT/zF \tag{A9}$$

with z, F, R, T, V having their usual meaning, implies a potential profile with the peak in the middle of the membrane (Läuger & Stark, 1970). This assumption is not crucial for the conclusions obtained in this article.

As N_1 and N_2 change with membrane potential, they have to be replaced by N_t, the overall sum of carriers.

The calculation of the overall sum, N_t, suffers from the fact that not all intermediates of the carrier cycle are known. A solution for this problem is found in the concept of "reserve factors" (Hansen et al., 1981; Gradmann, Hansen & Slayman, 1982): In a chain of reactions any intermediate N_j is completely defined by the two members at either end, which are N_1 and N_2 in Class-I models (*see* Fig. 2).

$$N_j = \frac{\kappa_{1j}}{\kappa_{j1} + \kappa_{j2}} N_1 + \frac{\kappa_{2j}}{\kappa_{j1} + \kappa_{j2}} N_2 = r_{1j}N_1 + r_{2j}N_2. \tag{A10a,b}$$

For $j = 3$, Eq. (A10) is obtained from Eq. (A6) for the steady-state condition $dN_3/dt = 0$.

The reserve factors allow the calculation of N_t

$$N_t = \sum_j r_{1j}N_1 + \sum_j r_{2j}N_2 = r_iN_1 + r_oN_2. \tag{A11a,b}$$

In most systems, the reserve factors r_{1j} and r_{2j}, and thus the overall reserve factors r_i and r_o, are still unknown. But as they are related to N_1 and N_2 by neutral reactions only (definitions of N_1 and N_2 in a Class-I model, *see* Fig. 2), they are at least constant during an I/V curve measurement. This very often enables a useful mathematical treatment as in this article.

The pseudo-2-state model of Fig. 1*C* is the obvious model for the calculation of single I/V curves. From its rate equations (similar to Eqs. A1 to A4) at steady state we obtain

$$N_2 = \frac{k_{12} + \kappa_{12}}{k_{21} + \kappa_{21}} N_1. \tag{A12}$$

Inserting Eqs. (A11b) and (A12) into Eq. (A7) leads to the general formula for the current in any Class-I model:

$$I = zFN_t \frac{k_{12}\kappa_{21} - k_{21}\kappa_{12}}{r_o(\kappa_{12} + k_{12}) + r_i(\kappa_{21} + k_{12})} \tag{A13}$$

with the voltage entering Eq. (A13) via k_{12} and k_{21} according to Eqs. (A8a,b).

The influence of the lazy-state L is seen, if the reserve factors are split into one part including all carriers within the transport cycle and another one accounting only for L:

$$r_i = r_i^0 + r_{1L} = r_i^0 + qr_{13} = r_i^0(1 + qr_{13}/r_i^0) \tag{A14a,b,c}$$

and similarly

$$r_o = r_o^0(1 + qr_{23}/r_o^0) \tag{A15}$$

q is introduced by means of Eq. (A5).

r_o^0 and r_i^0 are independent of the membrane potential and of the occupation of L, because only the rate constants between N_3 and N_i and N_3 are included in these reserve factors. Thus, they are constant in our experiments. The insertion of Eqs. (A14c) and (A15) into Eq. (A13) leads to

$$I = zFN_t \frac{k_{12}\kappa_{21} - k_{21}\kappa_{12}}{r_o^0(1 + qr_{23}/r_o^0)(\kappa_{12} + k_{12}) + r_i^0(1 + qr_{13}/r_i^0)(\kappa_{21} + k_{21})}. \tag{A16}$$

The curve shape of the I/V curve is changed in most cases, when carriers move into or out of L. This is especially seen from the positive and the negative saturation currents

$$I_{sat+} = zFN_t \frac{\kappa_{21}}{r_o} \text{ and } I_{sat-} = zFN_t \frac{\kappa_{12}}{r_i} \quad \text{(A17a,b)}$$

because according to Eqs. (A14c) and (A15) r_o and r_i suffer unequal changes with changes in q.
If

$$\frac{r_{13}}{r_i^0} = \frac{r_{23}}{r_o^0} \quad \text{(A18)}$$

then the factors in Eq. (A16) resulting from Eqs. (A14c) and (A15) are equal. In that case these factors could be merged into N_t. If the condition of Eq. (A18) holds, N_3 is in the "reaction-kinetic middle" between N_i and N_o, and the scaling factor, but not the curve shape is changed with the occupation of L.

For curve fitting of the lazy-state model (Fig. 2*B*) a different version of Eq. (A16) is used:

$$I = zFN_t \frac{k_{12}\kappa_{21} - k_{21}\kappa_{12}}{r_o^0(1 + xm)(\kappa_{12} + k_{12}) + r_i^0(1 + x)(\kappa_{21} + k_{21})} \quad \text{(A19a)}$$

$$I = zFN_t \frac{k_{io}\kappa_{oi} - k_{oi}\kappa_{io}}{(1 + xm)(\kappa_{io} + k_{io}) + (1 + x)(\kappa_{oi} + k_{oi})}. \quad \text{(A19b)}$$

In Eq. (A19b) the (only measurable) apparent rate constants indexed by i and o replacing 1 and 2 are used. These apparent rate constants are:

$$k_{io} = k_{12}/r_i^0 \qquad k_{oi} = k_{21}/r_o^0 \quad \text{(A20a,b)}$$
$$\kappa_{io} = \kappa_{12}/r_i^0 \qquad \kappa_{oi} = \kappa_{21}/r_o^0 \quad \text{(A20c,d)}$$
$$r_{i3} = r_{13}/r_i^0 \qquad r_{o3} = r_{23}/r_o^0 \quad \text{(A20e,f)}$$
$$N_i = N_1 r_i^0 \qquad N_o = N_2 r_o^0 \quad \text{(A20g,h)}$$

The comparison of Eqs. (A16) and (A19) shows that

$$xm = qr_{o3} \text{ and } x = qr_{i3}. \quad \text{(A21a,b)}$$

Rearrangement of Eqs. (A21a,b) leads to

$$m = \frac{r_{o3}}{r_{i3}} \quad \text{(A22a)}$$

which is a measure of the location of N_3. If $m = 1$, N_3 is in the reaction kinetic middle.

According to Eq. (A20b), x is a parameter which increases linearly with q (Eq. A3), and thus with the occupation of L.

$$x = \frac{k_{3L}r_{i3}}{k_{L3}}. \quad \text{(A22b)}$$

C. Distribution of Carriers between the Lazy-State L and the Transport Cycle

According to Eq. (A6)

$$N_3 = r_{13}N_1 + r_{23}N_2 \quad \text{(A23)}$$

and to. Eq. (A5), we obtain

$$L = qr_{i3}N_1r_i^0 + qr_{o3}N_2r_o^0 \quad \text{(A24)}$$

with r_{i3} and r_{o3} being defined by Eqs. (A20e,f).

The introduction of Eq. (A21) and of Eqs. (A20g,h) leads to

$$L = xN_i + xmN_o. \quad \text{(A25)}$$